Distributed Energy Resources: A Review, Modeling, and Cyber-Physical Potential of Solar and Wind Generation

Leen Al Homoud
Department of Electrical and Computer Engineering
Texas A&M University
College Station, TX
leen.alhomoud@ieee.org

Katherine Davis, *Senior Member, IEEE*
Department of Electrical and Computer Engineering
Texas A&M University
College Station, TX
katedavis@tamu.edu

***Abstract*—Over the last few decades, the need for renewable energy generation has been increasing rapidly. Much of this need stems from the necessity for cleaner energy sources that would heavily improve the quality of life for future generations. As such, this led to the rise of distributed energy resources (DERs), with a lot of focus on DER integration into the existing power grid. This integration comes with many research challenges centered on maintaining system reliability, power quality, resiliency, and security - opening the floor for highlighting the need for cyber-physical resilient energy systems. In this paper, we will perform a literature review on the different efforts made in modeling distributed energy resources and cyber-physical power systems. Additionally, we will introduce and develop models for solar and wind energy integrated into the IEEE 13 bus distribution network. The models are validated by studying and analyzing the bus voltage limits in comparison with the standards set by the American National Standards Institute (ANSI). The criticality of this work lies in its future purpose of aiding in cyber-physical analyses complementary to implementing a cyber-physical resilient energy management system.**

***Index Terms*—Distributed energy resources, photovoltaic systems, wind power, solar power, cyber-physical systems.**

I. Introduction

Distributed energy resources (DERs) have been the focus of power systems research for a few years now, as the integration of such resources poses many research challenges and questions that need to be answered to ensure a more sustainable future. These challenges arise due to three different characteristics of DERs, which are as follows:

1) The intermittent inherent nature of many DERs, such as solar and wind energy.
2) The two-way flow of communication that arises when DERs are integrated into the existing power grid.
3) The cyber-physical security vulnerabilities that emerge from the increased communications with DERs in the grid.

The intermittent nature leads to voltage management issues, as studied and discussed in [1] and [2]. Voltage control is an extensive research area in DERs as the integration of these resources results in voltage fluctuations that have disastrous impacts on the power grid, deteriorating the system stability and power quality [1]. Another important area of research includes the optimal location of distributed generation in the power grid, mainly in the distribution network, which is studied in [3]. Other challenges, according to [4], include, but are not limited to, reactive power support, fault ride-through capabilities, and non-dispatch-ability.

In addition to all these challenges, one main issue lies in ensuring the cyber-physical security of the system. This is essential as more vulnerabilities emerge with the integration of distributed energy resources. The idea of cyber-physical security lies in combining both the cyber and physical characteristics of the system to create a more resilient power system - generation, transmission, distribution, and consumer-side loads included. This resiliency is formatted as a concept of ensuring a resiliency life-cycle, as stated in [5]. The approach of a resilient life-cycle involves preparing for, enduring, responding to low-frequency high-impact events (such as threats), learning from such events, and planning the system better. The Cyber-Physical Resilient Energy Systems (CYPRES) project has developed an energy management system (EMS) that helps to run and study different cyber-physical grid scenarios by utilizing both the cyber-physical data and cyber-physical models [5], which will be discussed in section II-B.

This paper will focus on providing a literature review of different efforts in distributed energy resources modeling, which will be highlighted in section II-A. The literature review will then focus on the CYPRES project testbed and the importance of cyber-physical power systems, which will be in section II-B. After the literature review, we will focus on distribution network modeling with the integration of solar and wind energy. Section III will first introduce the IEEE 13 bus network in section III-A, and then move on to the solar and wind energy models in sections III-B and III-C, respectively. Once the modeling is complete, a time-series simulation is set up to run a few case studies, and the results are discussed and analyzed in section IV. Finally, the paper is concluded with a list of future work suggestions that include the implementation of these models in the existing CYPRES project testbed for cyber-physical security studies.

II. Literature Review

In this section, we will go over recent work in distributed energy resources modeling, such as voltage control and management issues [1], [2] and determining the optimal location of distributed generation [3]. Other challenges will also be discussed, as highlighted in [4]. We will also discuss the concept of cyber-physical power systems in existing literature, highlighting the CYPRES project [5] testbed.

A. Distributed Energy Resources

In [1], the authors provide a review on voltage control in a distributed and decentralized manner in the distribution network. They highlight that the need for voltage control comes from the intermittent nature of DERs that lead to quick voltage fluctuations in the system. Certain DERs, such as plug-in electric vehicles, can cause a sudden increase in load, which can drastically affect power quality. The existing voltage regulation devices at utilities are unable to respond quickly and efficiently to these sudden changes in voltage and loads. Therefore, it is important to research and study different control schemes and algorithms. To understand these algorithms, we would first need to define the voltage control problem. The authors describe this problem as one where the objective is to maintain the voltage within the standard voltage limits. The different methods to approach this problem are listed by [1] as distributed optimization, decentralized optimization, distributed cooperation, distributed adaptive control, distributed model predictive control, decision making, and hybrid methods.

From the methods above, distributed optimization is the only one capable of obtaining the global optimum. Additionally, the decentralized approach has the fastest computation time while risking possible control failure. Another important issue to highlight is that while both the distributed adaptive control and the distributed model predictive control can handle parameter disturbances, they are still computationally expensive. As a result, it can be concluded from work done in [1] that the algorithm for voltage control is heavily dependent on the goal and research question in mind.

In [2], Garzón et al. focus on studying the effects of the placement of a photovoltaic (PV) system in a distribution network on power flow and bus voltages. To do so, the authors worked on the IEEE 13 bus network, which is a distribution network model. The modeling was done on a software named OpenDSS, which is an open-source Distribution System Simulator (DSS). OpenDSS is known to be essential in studying and analyzing distributed energy integration into the distribution network [6]. Garzón et al. model a PV system and connect it to the IEEE 13 bus network. To run the simulation, both OpenDSS and MATLAB [7] were used to run the time-series simulation to perform the studies. The voltage limit references were based on the ones set by the American National Standards Institute (ANSI) [8]. This standard is named ANSI C84.1-2020, allowing a +/- 5% voltage difference, as shown in Figure 1 below. It also shows an acceptable range of voltages, which are still allowed despite going a little beyond the limits. Garzón et al. conclude that adding a PV system was useful to make up for a potential loss in generation - maintaining bus voltages within ANSI limits and supporting system recovery.

Utilization voltage limits according to ANSI C84.1-1 of 2006

	Utilization voltage limits	
	Optimal voltage range	**Acceptable voltage range**
Minimum	90%	86.7%
Maximum	105%	105.8%

Fig. 1. ANSI Voltage Limits [2]

In [3], Liang et al. focus on analyzing the capacity and location of distributed generation in the grid. This is essential as the incorporation of distributed generation into the power grid keeps increasing. To perform the studies, the OpenDSS software was utilized, in which a model of a 10 kV distribution network based in China was implemented. The authors focused on studying the effects on the voltages, power losses, and short-circuit currents in the system. The authors defined the head of the line as the bus closest to the substation and the end of the line as the bus that is the furthest from the substation. With that being said, after performing the studies, the authors concluded that the distributed generation of the PV systems could increase the voltage on the line if the PV system is placed at the head of the line. However, if reducing the voltage was required, the PV system would need to be placed at the end of the line. The PV system would also have to be placed at the end of the line to reduce power losses. Finally, placing the PV system at the head of the line helps to minimize the distributed generation effects on the short-circuit currents.

In the following two papers, the authors focused on developing algorithms to identify the different DERs connected in distribution networks. This work is essential as it helps in the planning and operation phases of smart distribution networks. In [9], Jaramillo et al. focused on identifying DERs by developing a supervised learning algorithm, which should predict and identify photovoltaic (PV) generation or electric vehicle (EV) loads. The authors successfully developed a k-Nearest Neighbors (k-NN) classification algorithm that can detect DERs. In [10], Weng et al. developed a graphical model algorithm that is data-driven and probability-based and were able to identify distributed generation sources successfully.

The authors in [11] and [12] focused on modeling a PV system and a storage element in the IEEE 34 bus distribution network on OpenDSS. Al Homoud et al. focused on developing a machine learning algorithm that can help detect cyber-physical anomalies. To train and develop the algorithm, the authors used OpenDSS to modify the existing IEEE 34 bus distribution network by adding a PV system and storage elements. Controllers were also modeled for the capacitors and voltage regulators in the system. Modeling is explained in more detail in [11]. In [12], the focus was on training a local anomaly detection algorithm called Local Outlier Factor (LOF), an unsupervised learning method. For training, yearly Monte Carlo simulations were run to create the training dataset. The algorithm was then tested on datasets that contained forged data, which comprised the testing dataset. For

evaluation, the authors used precision, recall, and F1-score values. With that being said, they were able to successfully detect anomalies, achieving a few false negatives.

B. Cyber-Physical Power Systems

In this section, we will briefly explain the CYPRES project testbed [13]. It is essential to highlight that, while this paper does not focus on cyber-physical security studies, it is still important to discuss the CYPRES project testbed to build a context for the criticality of this paper in future work applications, which will be discussed later on in section V.

The testbed is the Resilient Energy Systems Lab (RESLab), which includes cyber and physical models, as well as protection systems set in place to ensure resiliency. To model the cyber network, the Common Open Research Emulator (CORE) is used, which facilitates communication between different system devices. To model the physical grid, the Power World Dynamic Studio (PWDS) software is used, which allows for running real-time dynamic simulations of electrical transmission networks. To model the protection systems, both the PWDS software and SEL Real-Time Automation Controller (RTAC) are utilized, where the latter allows for hardware-in-the-loop studies and applications. The protocol used for all communication between the devices in the system is the Distributed Network Protocol 3 (DNP3). The general overview of the testbed is in Figure 2, which shows the architecture for one utility control center (UCC) and substation.

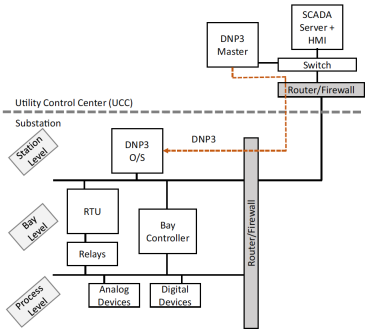

Fig. 2. RESLab Architecture Overview [13]

As shown in Figure 2, the Substation side contains the Process Level and the Bay Level. The Bay Level contains the control devices that would help to monitor the analog and digital devices at the Process Level. The most relevant aspect to highlight is the DNP3 communication between the DNP3 outstation at the Substation side and the DNP3 Master at the UCC side. The concept is that the DNP3 outstation is the data collection point from the real-time simulation of the physical system at the substation, which is facilitated by the PWDS software. This data is then pushed to the DNP3 Master, which successfully ensures the transfer of data from the substation all the way to the balancing authority. This is essential because the future work for this paper aims to connect the OpenDSS model to the DNP3 outstation and set up the communication flow, which is discussed in more detail in section V.

The U.S Department of Energy released a report in October 2022 discussing cybersecurity challenges surrounding DERs in the existing electric grid [14] that combines aspects of sections II-A and II-B. Essentially, the idea is that ensuring cybersecurity is not just a system requirement that is checked off after the systems are already in place. It should be an inherent characteristic of the system, establishing ”security by design” as the core aspect of the systems [14]. This is where the modeling work done in this paper comes into play. We are essentially taking into account the potential cyber-physical vulnerabilities of the system as it is built, where the ANSI voltage limits studies and analysis work is done.

III. Methodology

In this section, we will be introducing and discussing the IEEE 13 bus distribution network and highlighting its characteristics. We will then discuss and elaborate on the PV system and wind generation models that were added to the network. All the modeling work was done on OpenDSS [6].

A. Test Case

The test case used for incorporating the solar and wind models is the IEEE 13 bus network, which is a small-scale distribution network model created through the efforts of teams at IEEE Power and Energy Society (PES) [15]. This network operates at a nominal voltage of 4.16 kV. It is also characterized by the following [15]:

1) Heavily loaded network, with multiple spot loads and one distributed load. Loading is also unbalanced.
2) One voltage regulator at the substation.
3) Underground and overhead lines.
4) One in-line transformer and two shunt capacitors.

Figure 3 shows the IEEE 13 bus network with the additions of solar and wind generation, which will be explained in the following sections. The spot loads in the network are at buses 634, 645, 646, 652, 671, 675, 692, and 611. The distributed load is between buses 632 and 671. The two shunt capacitors are placed on buses 611 and 675. It is also good to note that a switch is modeled between buses 671 and 692. As there are no loads on bus 680, the solar and wind models will be integrated into that bus. It is also important to highlight that the modeling and analysis are done separately for each of those DERs, so both are not modeled at the same bus simultaneously. This eases the analysis process, as it will help us understand precisely how each type of DER affects the bus voltages.

B. Photovoltaic System Model

An overview of how the photovoltaic (PV) system is modeled in OpenDSS can be shown in Figure 4. The PV system is divided into three main parts, which are the PV array, the inverter, and the Norton Equivalent. The PV array collects solar energy that is transformed into a current, which is sent to the inverter to be converted to an AC current source. The Norton Equivalent then serves to provide a voltage difference that is supplied to that end of the system. Four curves are needed to model the PV system, which are:

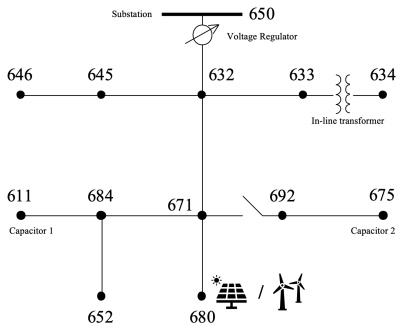

Fig. 3. IEEE 13 Bus Network with Wind and Solar Models

- Irradiance and Temperature Curves.
- PV Correction Factor vs. Temperature Curve.
- Inverter Efficiency vs. Power Curve.

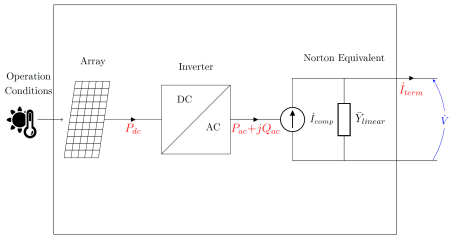

Fig. 4. PV System Block Diagram [6]

The first two curves were obtained from yearly irradiance and temperature data downloaded from the NSRDB: National Solar Radiation Database developed by the National Renewable Energy Laboratory (NREL) [16]. The NSRDB Viewer tool allows the user to select a location on the map and download the required data. The location selected for this work is an area in Texas, United States, at a latitude of 31.2 and a longitude of -98.61. The dataset collected in 2019 was used in this paper. The irradiance (W/m^2) and temperature ($^\circ C$) data were collected at increments of 5 minutes, which meant there was a total of 105,120 data points for each curve. For the irradiance, the clear-sky direct normal irradiance (DNI) values were considered for this model.

For determining the last two curves, a similar methodology was used in [11]. For the PV correction factor vs. temperature curve, four data points are sufficient enough to model the needed characteristics. As such, the four temperatures of $0^\circ C$, $25^\circ C$, $75^\circ C$, and $100^\circ C$ were considered, with $25^\circ C$ set as the base temperature. The base temperature was then assigned a unity PV correction factor. To calculate the remaining PV correction factors, the following formula was used [11]:

$$CorrectionFactor = \frac{P(t)}{P_{STC}} \tag{1}$$

where, P(t) is the power calculated at a specific temperature and P_{STC} is the power at standard test conditions (STC).

To calculate P(t), we used a PV module datasheet, as described in [11]. The PV module datasheet was obtained from a company named ENF Solar [17]. From this datasheet, we obtained the power and temperature at STC, the temperature coefficient, and the temperature. Once these values were collected, the formula below was used to calculate P(t) [11]:

$$P(t) = P_{STC} \cdot (1 - C \cdot (T - T_{STC})) \tag{2}$$

where, the power at STC (P_{STC}) is 390 W, the temperature coefficient (C) is $-0.28\%/^\circ C$, and the temperature at STC is $25^\circ C$. Using all the values defined above and equations 1 and 2 respectively, the data points for the PV correction factor vs. temperature curve are calculated and shown in Table I.

Lastly, the inverter efficiency vs. power curve is obtained from inverter efficiency values from the California Energy Commission [18], as explained in [11]. The values were collected for the ABB PVI-3.0-OUTD-S-US-A inverter, which is defined as a 3 kW, 208 Vac grid support utility-interactive inverter with an arc detector, as stated in [11] and [18]. The values are shown in Table I.

TABLE I
DATA FOR PV SYSTEM INPUT CURVES

PV Correction Factor vs. Temperature Curve		**Inverter Efficiency vs. Power Curve**	
Temperature	**Correction Factor**	**Power**	**Inverter Efficiency**
$0^\circ C$	1.07	0.1	93.3%
$25^\circ C$	1	0.2	95.9%
$75^\circ C$	0.86	0.3	96.4%
$100^\circ C$	0.79	0.4	96.4%
-	-	0.5	96.2%
-	-	0.6	95.8%

Last but not least, an important parameter that was considered when modeling the PV system was the power at the maximum power point (P_{mpp}), which is set at 346.6128 kW, making the PV penetration at 10% since the total real power load on the IEEE 13 bus network is 3466.128 kW [15].

C. Wind Generation Model

To model wind generation in OpenDSS, a wind turbine power output profile is needed to model the wind turbine characteristics relating to wind speed and energy. The power output profile used in this model is an example file [19] that contains actual power output measurements from a Vestas V47 turbine rated at 660 kW [20]. The wind output file is used as a multiplier function that is normalized and then multiplied by the nominal power (kW) of the system model to generate a profile [20]. With that being said, it is important to highlight that the rated kW of the wind generator modeled is 500 kW, which is around 14.4% of the total 3466.128 kW load consumption of the IEEE 13 bus network.

IV. RESULTS

In this section, we will go over the simulation setup requirements, which include, but are not limited to, assigning yearly load profiles to the different loads in the system, which are obtained from the REopt web tool [21] developed by the National Renewable Energy Laboratory (NREL). Once the time-series simulation is set up, we run a few case studies

to understand better how the bus voltages fluctuate as the PV and wind energy are separately integrated into the system. The ANSI bus voltage limits introduced and discussed in Section II-A will be used as a reference; specifically, the voltage limit values highlighted by Garzón et al. [2] in Figure 1.

A. Simulation

To set up the simulation, the mode was set to yearly on OpenDSS with a timestep of 5 minutes, which matches the format of the irradiance and the temperature profiles. The reason this is done is that OpenDSS can interpolate any input files that have a timestep higher than the simulation timestep. For example, the yearly load profiles that will be discussed are collected hourly. The values will be interpolated to match the format of the time-series simulation. The total number of points collected at each time-series simulation is 105,120 for each element monitored. Monitoring on OpenDSS is equivalent to adding a sensor that collects data from an element in a hardware system environment. As such, monitors were placed on all the buses to collect the voltage measurements.

As mentioned earlier, the load profiles were collected from [21], which was also done in a similar manner in [11]. The reason load profiles are collected is that the IEEE 13 bus network loads are static, and we need dynamic load profiles to run the time-series simulations for the models and case studies. Since we have a total of 9 loads in the system (8 spot loads and 1 distributed load), we will need 9 yearly load profiles. The location entered on REopt [21] is Texas, USA. The different load profiles that were collected were:

1) Critical loads: Hospital and outpatient health care.
2) Residential load: Midrise apartment.
3) Commercial loads: Large office space, primary school, full-service restaurant, retail store, and supermarket.
4) Industrial load: Warehouse.

B. Case Studies

Once the time-series simulation settings were complete, three case studies were run to analyze the behavior of the IEEE 13 bus network. The three case studies that were run were a time-series simulation of the test case with no DER integration, a simulation with only PV system integration, and a simulation with only wind integration. All the three-phase bus voltages were collected, and the maximum and minimum voltages for each were recorded respectively in Table II.

In the first case study, an important observation to highlight is that all voltages are within the allowed ANSI voltage limits [8]. One system characteristic to highlight is that it can be seen that the buses closer to the substation (646, 645, 632, and 633) observe high values of both the minimum and maximum voltages, where the bus voltages never go below 1 p.u. A reason for this could be location-specific, as they are close to the substation. As you go farther from the substation, the voltage values lower, with the lowest voltage of 0.93 recorded at both buses 652 and 680. Such an observation means that ensuring the cyber-physical security of such buses is critical, as a minor attack could lead to a disastrous voltage deviation. It was also interesting to notice that buses 671, 680, and 692 all have the same voltage values for all three phases. As these buses are in the same region, those are reasonable values, especially since a switch is between buses 671 and 692.

In the second case study, the most important observation to note is that the integration of the PV system impacted the different voltage phases differently, where each phase demonstrated the same behavior. In phase A, it was noticed that the addition of the PV system increased the minimum voltage values for the buses close to the substation (646, 645, 632, 633, and 634). This means that voltage values are rising, which could be alarming, except, in this case, only the lower values are increasing, which is acceptable as the values remained within the ANSI voltage limits. For the buses farther from the substation (611, 684, 652, 671, 680, 692, and 675), their minimum voltage values decreased, causing alarm as they were deviating from the ANSI voltage limits. In phase B, the effects were mainly seen on the maximum voltage values instead of the minimum values, with a reduction in all voltage values, which is desirable. In phase C, voltage reductions were seen in both the maximum and minimum values. Lastly, it is essential to highlight that buses 671, 680, and 692 no longer have the same voltage values, which is an expected outcome as the PV system was added to bus 680.

In the third case study, the most important observation is that the integration of the wind generation caused the voltages in phases A and B to behave similarly, while phase C voltages showcased different patterns. In phases A and B, the maximum voltage values decreased while the minimum voltage values increased for all the buses near the substation. This is a very desirable characteristic because it means that both values are slowly converging to unity, taking into account that all voltages remained within the ANSI voltage limits, which is the case for all of these buses except 632 and 633 since their minimum voltage was already above 1 p.u. For the buses far from the substation, their phase A and B maximum and minimum voltages all increased. This is acceptable for phase A voltages as they are all within limits; however, the phase B voltages for the buses far from the substation are all around 1.6 p.u., which is above the ANSI voltage limits, making it critical as it can potentially cause cyber-physical vulnerabilities. In phase C, the minimum and maximum voltages decreased for the buses close to the substation and increased for the buses placed far away while remaining within voltage limits.

V. Conclusions and Future Work

The contributions of this paper are twofold. First, we provided a literature review on distributed energy resources and the efforts to deal with challenges related to DER integration, such as voltage control and management, reactive power support, and optimal DER placement. We focused on the importance of looking at DERs in a cyber-physical context, highlighting the importance of incorporating the ”security by design” concept. Second, we modeled solar and wind generation in an IEEE 13 bus network and studied the system behavior by analyzing the bus voltages with respect to the

TABLE II
CASE STUDIES SIMULATION RESULTS

Bus Number	Phase A (p.u. voltage)			Phase B (p.u. voltage)			Phase C (p.u. voltage)		
-	No DERs	PV	Wind	No DERs	PV	Wind	No DERs	PV	Wind
646	1.01657, 0.99657	1.01657, 0.99657	1.01645, 0.99679	1.03645, 1.01315	1.03590, 1.01315	1.03227, 1.01337	-	-	-
645	1.01783, 0.99943	1.01783, 0.99943	1.01758, 0.99940	1.03838, 1.01448	1.03838, 1.01448	1.03399, 1.01477	-	-	-
632	1.03304, 1.00595	1.03304, 1.00634	1.03286, 1.00699	1.04961, 1.02112	1.04779, 1.02112	1.04469, 1.02155	1.01903, 1.00175	1.01903, 1.00175	1.01889, 1.00170
633	1.03195, 1.00081	1.03195, 1.00148	1.03166, 1.00185	1.048332, 1.01867	1.04644, 1.01867	1.04336, 1.01912	1.01651, 0.99908	1.01650, 0.99908	1.01636, 0.99903
634	1.01916, 0.96455	1.01916, 0.96596	1.01825, 0.96552	1.03013, 0.99992	1.02819, 0.99992	1.02506, 1.00037	0.99771, 0.97994	0.99770, 0.97994	0.99756, 0.97989
611	0.991932, 0.94274	0.991928, 0.93886	0.997199, 0.94345	-	-	-	-	-	-
684	0.992615, 0.94612	0.992611, 0.94241	0.997599, 0.94694	-	-	-	-	-	-
652	1.02041, 0.93987	1.02041, 0.93779	1.02285, 0.94171	-	-	-	-	-	-
671	1.02472, 0.95034	1.02472, 0.94832	1.02699, 0.95223	1.06657, 1.02775	1.06298, 1.02775	1.06258, 1.02867	0.99332, 0.94948	0.99332, 0.94595	0.99802, 0.95041
680	1.02472, 0.95034	1.02472, 0.94703	1.02833, 0.95272	1.06657, 1.02775	1.06244, 1.02775	1.06306, 1.02885	0.99332, 0.94948	0.99351, 0.94466	0.99911, 0.95098
692	1.02472, 0.95034	1.02472, 0.94832	1.02699, 0.95223	1.06657, 1.02775	1.06298, 1.02775	1.06258, 1.02867	0.993323, 0.94948	0.993318, 0.94595	0.99802, 0.95041
675	1.02201, 0.93992	1.02201, 0.93784	1.02447, 0.94176	1.06911, 1.02991	1.06552, 1.02991	1.06509, 1.03082	0.990637, 0.94852	0.990629, 0.94512	0.99518, 0.94953

ANSI voltage limits. The criticality of this work lies in its future purpose of aiding in cyber-physical analyses complementary to implementing a cyber-physical resilient energy management system. Future work includes integrating the models built in this paper into the RESLab testbed to run cyber-physical security analyses and scenarios that ensure a resiliency life-cycle approach. In conclusion, the work in this paper serves as a stepping stone to a future of cyber-physically resilient distributed energy resources and systems.

ACKNOWLEDGMENT

The work described in this paper was supported by funds from the US Department of Energy Cybersecurity for Energy Delivery Systems program under award DE-OE0000895.

REFERENCES

[1] K. E. Antoniadou-Plytaria, I. N. Kouveliotis-Lysikatos, P. S. Georgilakis, and N. D. Hatziargyriou, "Distributed and decentralized voltage control of smart distribution networks: Models, methods, and future research," *IEEE Transactions on smart grid*, vol. 8, no. 6, pp. 2999–3008, 2017.

[2] J. A. R. Garzón, D. J. G. Tristancho, and F. C. E. González, "Impact of changing location and power of a pv system in electrical distribution networks, integrating matlab and opendss," *DYNA: revista de la Facultad de Minas. Universidad Nacional de Colombia. Sede Medellín*, vol. 85, no. 205, pp. 125–131, 2018.

[3] C. Liang, H. Jun, W. Yiran, T. Jian, L. Hong, G. Sanrong, and W. Yin, "Analysis of access location and capacity of distributed generation based on opendss," in *2018 China International Conference on Electricity Distribution (CICED)*. IEEE, 2018, pp. 2264–2268.

[4] M. Shafiullah, S. D. Ahmed, and F. A. Al-Sulaiman, "Grid integration challenges and solution strategies for solar pv systems: A review," *IEEE Access*, 2022.

[5] K. Davis, "An energy management system approach for power system cyber-physical resilience," *arXiv preprint arXiv:2110.03451*, 2021.

[6] EPRI. What is OpenDSS? [Online]. Available: https://www.epri.com/pages/sa/opendss

[7] MathWorks. MATLAB. [Online]. Available: https://www.mathworks.com/products/matlab.html

[8] ANSI. American national standard for electric power systems and equipment—voltage ratings (60 hz). [Online]. Available: https://www.nema.org/standards/view/American-National-Standard-for-Electric-Power-Systems-and-Equipment-Voltage-Ratings

[9] A. F. M. Jaramillo, J. Lopez-Lorente, D. Laverty, J. Martinez-del Rincon, and A. M. Foley, "Identification of distributed energy resources in low voltage distribution networks," in *2021 IEEE PES Innovative Smart Grid Technologies Europe (ISGT Europe)*. IEEE, 2021, pp. 1–6.

[10] Y. Weng, Y. Liao, and R. Rajagopal, "Distributed energy resources topology identification via graphical modeling," *IEEE Transactions on Power Systems*, vol. 32, no. 4, pp. 2682–2694, 2016.

[11] S. H. Bayes, L. Al Homoud, and R. Reghunath, "Cyber-physical defense in smart distribution networks," Bachelor's Thesis, Texas A&M University, 2021.

[12] L. Al Homoud, R. Reghunath, S. Bayes, A. Peerzada, K. Davis, and R. S. Balog, "Cyber-physical defense in smart distribution networks," in *2021 North American Power Symposium (NAPS)*. IEEE, 2021, pp. 1–6.

[13] A. Sahu, P. Wlazlo, Z. Mao, H. Huang, A. Goulart, K. Davis, and S. Zonouz, "Design and evaluation of a cyber-physical testbed for improving attack resilience of power systems," *IET Cyber-Physical Systems: Theory & Applications*, vol. 6, no. 4, pp. 208–227, 2021.

[14] DOE. Cybersecurity considerations for distributed energy resources on the u.s. electric grid. [Online]. Available: https://www.energy.gov/eere/articles/doe-cybersecurity-report-provides-recommendations-secure-distributed-clean-energy

[15] IEEE. IEEE PES test feeder. [Online]. Available: https://cmte.ieee.org/pes-testfeeders/resources/

[16] NREL. Nsrdb: National solar radiation database viewer. [Online]. Available: https://nsrdb.nrel.gov/data-viewer

[17] ENF. Maxima gxb 390 pv module. [Online]. Available: https://www.enfsolar.com/pv/panel-datasheet/crystalline/40186

[18] C. E. Commission. Grid support solar inverter list. [Online]. Available: https://www.energy.ca.gov/media/2365

[19] EPRI. Opendss examples: Wind. [Online]. Available: https://github.com/tshort/OpenDSS/tree/master/Distrib/Examples/Manual

[20] EPRI. Opendss discussion. [Online]. Available: https://sourceforge.net/p/electricdss/discussion/861976/thread/768a1cd7/

[21] NREL. Reopt: Renewable energy integration & optimization tool. [Online]. Available: https://reopt.nrel.gov/tool/